Techniques for Deep Sea Near Bottom Survey Using an Autonomous Underwater Vehicle

Dana R. Yoerger[1], Michael Jakuba[1], Albert M. Bradley[1], and Brian Bingham[2]

[1] Woods Hole Oceanographic Institution dyoerger@whoi.edu, mjakuba@alum.mit.edu, abradley@whoi.edu
[2] Franklin W. Olin College of Engineering bbing@olin.edu

Summary. This paper reports the development and at-sea deployment of a set of algorithms that have enabled our autonomous underwater vehicle, ABE, to conduct near-bottom surveys in the deep sea. Algorithms for long baseline acoustic positioning, terrain-following, and automated nested surveys are reported.

1 Introduction

This paper reports navigation algorithms that enable an underwater vehicle to accomplish fully autonomous scientific surveys in the deep sea. These algorithms allow the vehicle to determine its position, to bottom-follow (maintain a constant height above seafloor terrain) and avoid obstacles, and to autonomously focus on the highest value parts of a survey.

Scientific exploration of the deep sea has traditionally been performed using inhabited submersibles, towed vehicles, and tethered remotely operated vehicles (ROVs). Autonomous underwater vehicles (AUVs) have begun to replace these vehicles for mapping and survey missions. Autonomous vehicles complement the capabilities of these existing systems, offering superior mapping capabilities, improved logistics, and improved utilization of the surface support vessel. AUVs are particularly well suited to systematic preplanned surveys using sonars, in situ chemical sensors, and cameras in the rugged deep sea terrain that is the focus of many scientific expeditions. Inhabited submersibles and ROVs remain the only option for manipulation tasks such as sampling, deploying and recovering experiments on the seafloor, detailed inspection, and servicing subsea instruments; however, high resolution maps from AUVs can facilitate these tasks.

Figure 1 shows the Autonomous Benthic Explorer (ABE), a 6000 m autonomous underwater vehicle that our team has been developing and deploying for fine-scale quantitative survey and mapping of the seafloor. ABE can survey at constant depth or bottom-follow even in rugged terrain, and it can

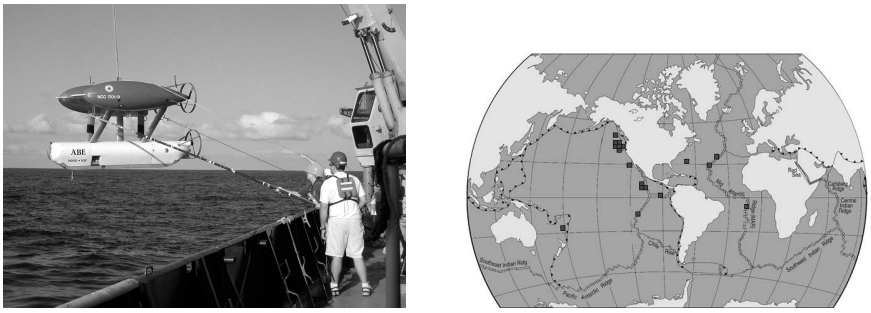

Fig. 1. Operations with the Autonomous Benthic Explorer (ABE): (**left**) ABE being recovered; (**right**) world map depicting ABE's 155 science dives. To date, ABE has surveyed a distance of over 2500 km in over 1300 h of bottom-time. The average depth of these dives was over 2000 m

autonomously determine its position and drive tracklines with a precision on the order of several meters. ABE carries a variety of sensors, including scanning and multibeam sonars; a magnetometer; a digital still camera; two sets of pumped conductivity and temperature probes; an acoustic Doppler current profiler (ADCP); several chemical sensors for hydrothermal plume mapping; and occasional mission-specific instrumentation. ABE's shape and thruster placement allow it to maintain control over a wide range of speed, and to stop or back up if necessary to avoid obstacles.

ABE descends to the seafloor with the aid of a descent weight. ABE glides in a controlled spiral trajectory to ensure that it reaches the desired starting point without consuming significant battery energy. After reaching the seafloor and performing a series of checks, ABE releases its descent weight to become neutrally buoyant and begins its survey. Throughout the dive, including descent, ABE uses acoustic long-baseline (LBL) transponder navigation and, when in range of the bottom (< 300 m), bottom-lock acoustic Doppler measurements to determine its position and velocity.

A dive can consist of a mix of hydrothermal plume survey at constant depth, sonar and magnetics survey following the seafloor (at heights of 50–200 m), and digital photography (height of 5 m). ABE usually surveys until its batteries are depleted (between 15 and 30 hours depending on sensor payload and terrain). At the end of its dive, ABE releases its ascent weight to become positively buoyant and returns to the surface.

The remainder of this report is organized as follows: Sect. 2 summarizes scientific survey tasks that have motivated our AUV work, Sect. 3 reports an algorithm for acoustic positioning, Sect. 4 reports methods for terrain-following and obstacle avoidance, Sect. 5 reports a technique for automated nested survey, and Sect. 6 presents a brief summary and conclusion.

2 Precisely Navigated, Coregistered AUV Surveys

Proximity to the seafloor, precise navigation, robust control, and coregistered sensors permit an AUV to characterize the seafloor and the near-bottom environment with complementary sensing modalities on the meter-scale. This section summarizes scientific work in which ABE-derived bathymetric maps, magnetics maps, digital photos, and hydrographic maps have played critical enabling roles.

Meter-scale bathymetric and magnetic maps made using ABE have provided geologists and geophysicists with new perspectives on important seafloor processes. Combined magnetics and bathymetric maps show crustal magnetization, which permits the age and thickness of lava flows to be determined. Combined maps have also been used to identify volcanic features such as lava flow units [1], delimit their fronts, and estimate their thicknesses [2, 3]. Meter-scale bathymetric maps show tectonic features such as faults with great clarity, even enabling them to be resolved into multiple components [4]. In other cases, these maps have revealed the relationship between tectonic features and morphology, such as volcanic domes [3], and hydrothermal vents [1]. ABE bathymetric maps have proved to be of sufficient detail and precision for one collaborator to reconstruct the tectonic history of a rift valley by computationally removing faults [5]. The result revealed a dome-like structure from which the valley evolved. On a recent cruise to the Atlantis Massif, detailed renderings of faults and the hydrothermal structures provided critical clues as to the mechanisms controlling the hydro-geology at the newly discovered Lost City hydrothermal vent site [6]. Digital photographs of the seafloor from ABE have provided details of lava flow types and effusion rates [3], sediment cover, and the distribution of benthic organisms.

Water column data from ABE yields indications of hydrothermal plume activity and has been used to estimate heat flux from known hydrothermal vent sites, and to locate undiscovered sites on the seafloor. To estimate the heat flux from vent fields on the Juan de Fuca Ridge in the Northeast Pacific (47°54′ N, 129°10′ W) [7], ABE measured temperature, salinity, and three-axis water velocity while repeatedly executing a tight grid pattern above the field [8]. Recently ABE located and preliminarily characterized several previously unmapped hydrothermal sites on the Eastern Lau Spreading Center (ELSC) south of Tonga (21°08′ S, 175°12′ W) [9]; and on the Southern Mid Atlantic Ridge (SMAR) north of Ascension Island (7°57′ S, 14°22′ W) [10]. In each case, we started with clues provided by towed systems that indicated a vent site within several kilometers. ABE then executed a three-dive sequence [9, 10] of grid patterns at increasing finer scales and increasingly close to the seafloor. To plan each dive, the scientific party carefully scrutinized the data from the previous dive along with any available ancillary data.

These vent prospecting missions capitalized on ABE's ability to conduct precisely navigated surveys at scales O (m–km), to operate over rugged terrain, and relied on nearly all of ABE's sensing modalities. Figure 2 shows

tracklines from sequence of dives designed to locate and survey a vent site on ELSC along with a sampling of the variety of data products acquired and used to plan each stage of the dive sequence. ABE mapped plume activity (temperature, optical backscatter, and reduction-oxidization potential (eH) [11]) to pinpoint the locations of plumes emanating from the field, built fine-scale bathymetric maps of the vent fields and surrounding environment, and finally photographed the vent structures and animal populations.

The remainder of this paper presents the underlying algorithms that enabled ABE to perform this work.

3 Real-Time Long Baseline Acoustic Navigation

Acoustic navigation from a set of seafloor transponders [13, 14] provides a critical capability for a seafloor mapping AUV. By georeferencing transponder location using GPS, the vehicle's position on the globe can be determined to within a few meters.

Long-baseline (LBL) positioning refers to the determination of position via interrogation of two or more fixed transponders separated by large distances (long baselines). The transponders all listen for a particular interrogation code and then reply immediately with their own unique codes. An AUV can determine its own position within a subsea LBL net as follows:

1. Before the vehicle is launched, an array of two or more acoustic transponders are moored near the seafloor. Their position and depth are determined by concurrently measuring acoustic travel times between each transponder and a number of different GPS-referenced vessel positions.
2. After launch, the vehicle repeatedly interrogates the transponders on a regular cycle and measures the time between the outgoing interrogation code and incoming replies from each transponder.
3. From these travel times, slant ranges to each transponder are computed using knowledge of the local sound speed profile, and are then projected onto the horizontal plane with knowledge of vehicle depth.
4. The horizontal position of the vehicle is then determined either through deterministic trilateration (two ranges received; relative position of baseline known), or through a nonlinear least-squares calculation (three or more ranges received).

Figure 3 shows acoustic travel time and range data from an ABE dive that illustrates many of the difficulties in autonomously processing LBL data. The upper panel of the figure shows many returns that do not correspond to the direct, round-trip path between transponder and vehicle. Some of these returns are distributed somewhat randomly, while others are systematic. The systematic incorrect returns correspond to paths that include either one or two reflections off the surface, so called bounce paths. These could be used for positioning if properly identified [15]. Returns from the previous cycle that

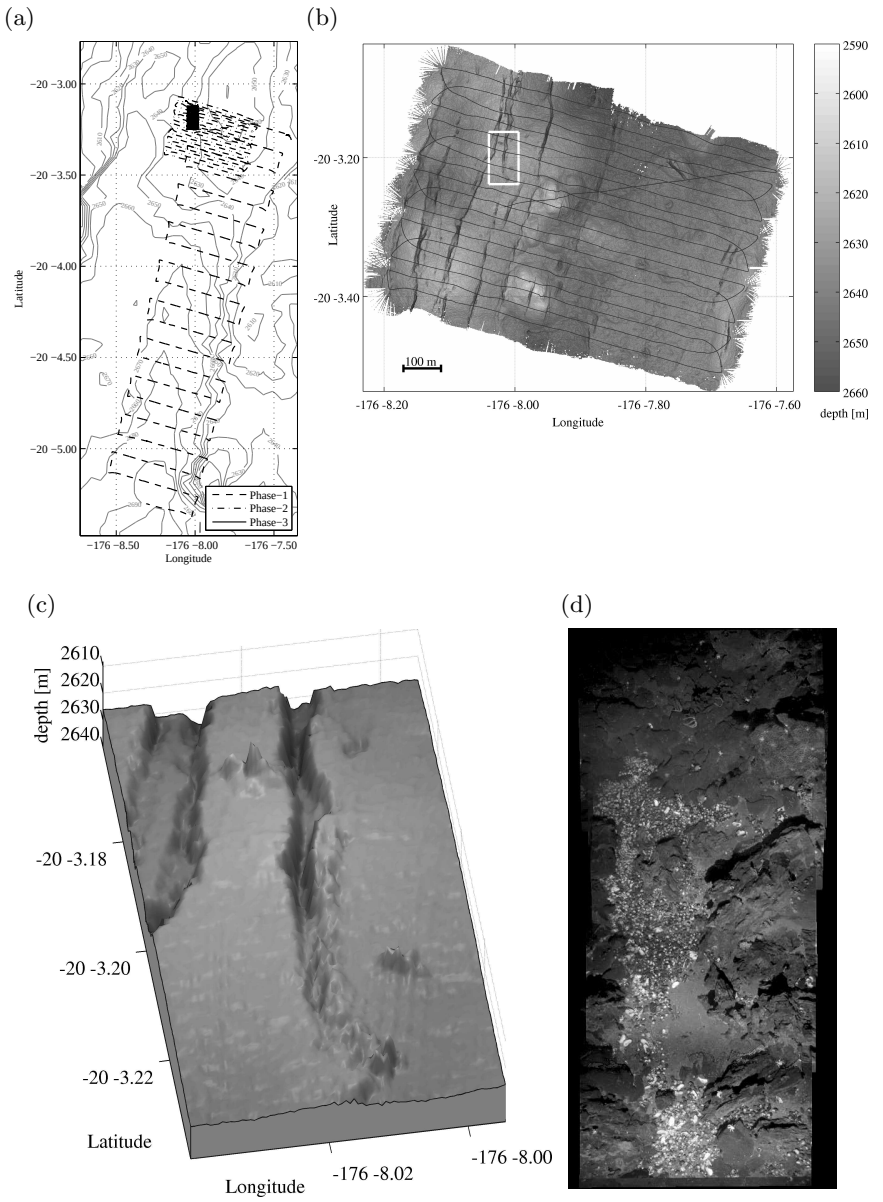

Fig. 2. Data products from a series of nested surveys whose purpose was to locate the source vent field of a hydrothermal plume near on the ELSC: (**a**) vehicle tracklines from the four nested surveys; (**b**) multibeam bathymetry overlain with vehicle tracklines; (**c**) closeup of bathymetry showing spires of hydrothermal origin (no vertical exaggeration); (**d**) photomosaic created automatically [12] from six individual photographs. We relied primarily on water column hydrothermal tracer data (not shown) to drive the design of each survey stage.

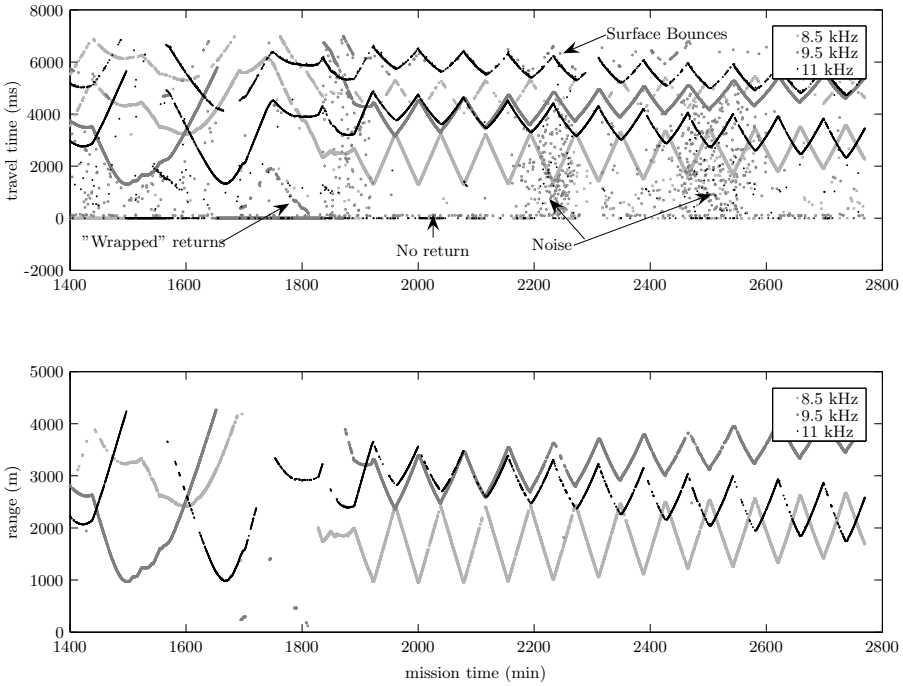

Fig. 3. Acoustic travel-time processing for long-baseline navigation: (**top**) raw acoustic travel times from three transponders, indicated by color, received by the vehicle during a survey operation; (**bottom**) filtered ranges computed by the vehicle in real-time. The labels indicate many of the pathologies of long baseline data: surface bounces, wrapped returns, missed returns, and nonstationary noise. The filtered results show that the median test and range gates in ABE's LBL navigation algorithm (Fig. 4) have largely rejected systematic, but incorrect returns from bounce paths and from previous cycles (wrap-around), and have also rejected most random, unsystematic returns

exceed the cycle period show up as short, consistent ranges (wrap-around). Reflections from terrain can provide consistent, incorrect returns as well. The distribution of unsystematic, random returns can change dramatically over the course of a dive, and we have even seen periods of uncorrelated returns due to active interrogation of the transponders by marine mammals. In summary, LBL range data is systematically corrupted by noise processes with non-Gaussian, nonstationary error distributions.

Because of these inherent difficulties, our LBL algorithm for autonomous AUV navigation (Fig. 4) emphasizes reliability over accuracy. The algorithm is self-starting and recovers gracefully from long periods of bad data. For instance, if the algorithm calculates a bad position due to unanticipated cir-

cumstances (e.g. a consistent reflection off a steep cliff), the computed position returns quickly to the correct position when the anomalous condition passes.

Much of the algorithm's reliability derives from the use of a median test for range consistency and from range gates that eliminate consistent bounce paths. These tests prevent most incorrect ranges from entering into fix computation. Both the capabilities and limitations of this portion of the algorithm are evident in the lower panel of Fig. 3. The indirect and wrap-around returns have been rejected as have nearly all the random returns. Even dense sections of noisy returns result in only a few bad ranges being accepted, and these single returns were rejected by the residual test when the fix was computed. The weakness of the median test is also evident: when the percentage of good ranges drops to near 50% or lower, the median test drops most ranges. Despite this weakness, we employ the median test for its predictability and ability to recover quickly from extended periods of bad data.

When the vessel is close enough to the vehicle, we observe the vehicle's position from the support vessel by monitoring the arrival time of the interrogation pulse from the vehicle and the corresponding replies from the transponders. This process is simplified if the time at which the interrogation is initiated at the vehicle is known. ABE's LBL cycle is controlled by a precise clock (accurate to 2 parts in 10^7, i.e. a drift of about 1 ms/h). From the vessel, we periodically interrogate a separate transponder on the vehicle to measure the slant range to the vehicle. Comparing this range to that implied by the interrogation pulse allows the start time of the acoustic cycle to be determined and any clock drift to be tracked.

4 Bottom-Following and Obstacle Avoidance

To execute mapping missions successfully, ABE must drive commanded tracklines and avoid unexpected obstacles. On seafloor imaging dives, ABE must also follow the seafloor at a prescribed height to ensure proper sonar (height: 50–200 m) and camera (height: 5 m) performance. Bottom-following and obstacle avoidance become especially difficult during photographic surveys, as the vehicle must cope with steep-sided features such as hydrothermal spires and scarps that are many times the nominal survey height (Fig. 1(c)). Spires and volcanic collapse pits frequently have overhanging structures that present a substantial threat, as the vehicle has no up-looking sonars and could become trapped.

Our a priori knowledge of the seafloor bathymetry is rarely sufficient to permit preplanning, therefore ABE's terrain-following algorithm (Fig. 6, left panel) relies strictly on real-time height data from three different sonar devices (two down-looking, one forward looking). The algorithm uses the height data to command the set-point for the depth controller, which remains active since the depth sensor is more reliable than the bottom-finding sonars. The depth setpoint is varied to keep the height off bottom within a prescribed depth

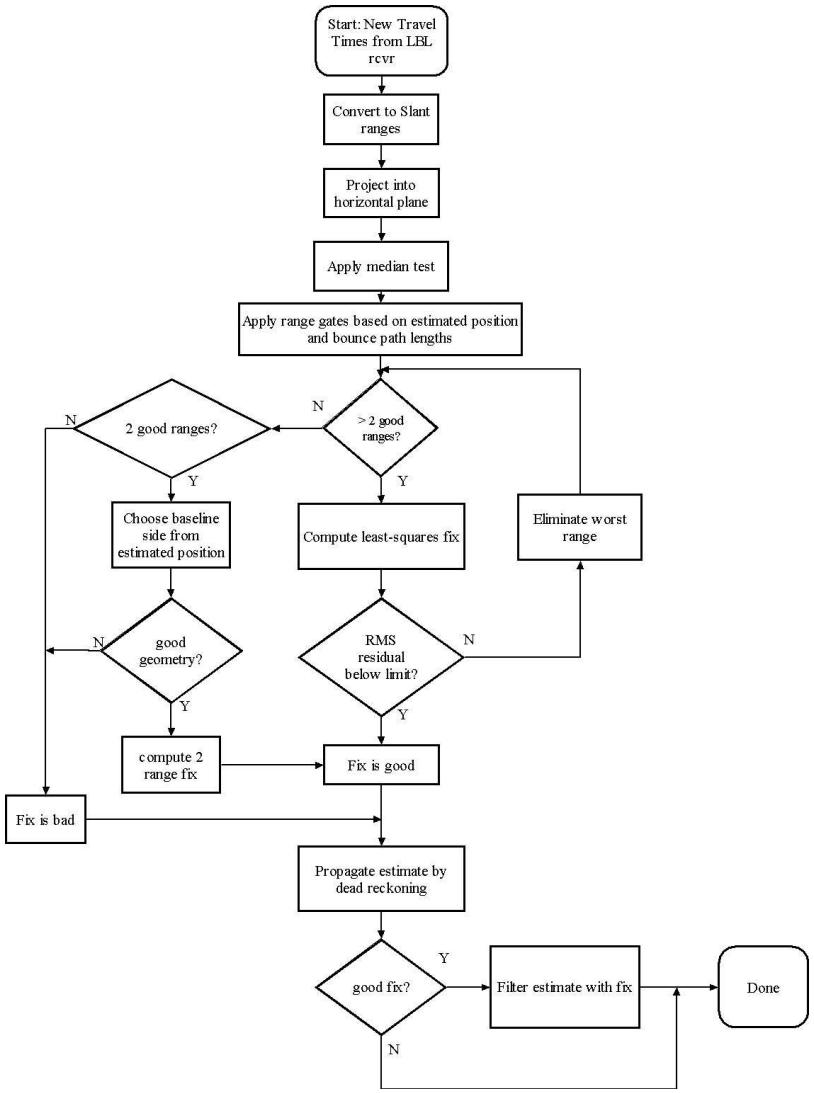

Fig. 4. Block diagram of our long baseline acoustic navigation processing algorithm. After converting travel times to ranges, a median test eliminates ranges that lack consistency over time. Consistent ranges may still be excluded before entering into the fix-computation portion of the algorithm if they fall outside of range gates derived from estimated position and expected bounce path lengths. Fixes are then computed with all available ranges; if three or more ranges are available, a least-squares solution is computed. Before a computed fix finally enters the vehicle's state estimate, it is checked for good transponder/vehicle geometry and sufficiently low residual error.

envelope. The envelope is established based on the desired depth, the desired height off bottom, and a prescribed thickness. The algorithm recomputes the envelope at each iteration based on the shortest of all reported ranges; however, it updates the depth setpoint only when the setpoint strays outside the envelope. When this happens, the algorithm recenters the commanded vehicle depth setpoint within the current envelope.

Tighter envelopes require the commanded vehicle position to follow the terrain more closely, but this requires increased vertical thruster activity and increases power consumption. When climbing or descending steadily, the depth set-point advances in steps. Additionally, forward thrust is reduced when the vehicle cannot change depth rapidly enough to stay in the envelope. Large deviations from the prescribed envelope, such as might be caused by the sudden proximal detection of a hydrothermal spire, cause the vehicle to reduce or even reverse forward thrust. The tight coupling between forward thrust and ABE's bottom-following and obstacle-avoidance performance takes advantage of ABE's ability to maintain control over a wide speed range. Figure 6 shows an example of bottom-following performance during a sonar survey at a nominal height of 40 m with a 10 m envelope.

5 Automated Nested Survey

This section describes our approach to data-driven nested survey for increasing the yield of high value data from unexplored hydrothermal vent fields. The critical component is a mapping algorithm (Fig. 7) that condenses hydrographic data acquired by our vehicle into a compact, two-tiered spatial representation of seafloor regions likely to contain active hydrothermal vents. We have implemented and field-tested the algorithm on near-bottom photosurveys. After completing the preplanned portions of these dives, ABE used maps constructed by the algorithm to plan additional tracklines over actively venting hydrothermal structures. These autonomously-directed additional surveys yielded improved coverage over high-value targets at a fraction of the cost of additional dives. Additional dives would have been necessary had human interpretation of the data been required.

The first tier representation produced by the algorithm consists of multiple fixed-length sorted lists of hydrographic measurements classified as indicative of hydrothermally altered water, relative the rest of each data set. Prior to classification, the raw data are filtered in time to enhance signals associated with venting, to compensate for sensor dynamics, and to reduce noise. For convenience, we filter the data such that large positive values cause measurements to be selected. As each new measurement arrives, its filtered value is compared with the least positive member in the corresponding list. Favorable comparisons cause the new measurement to be stored along with the vehicle's current location and the original list member to be discarded. This component of the algorithm is executed iteratively, with list-lengths set to $O\,(0.1\%)$

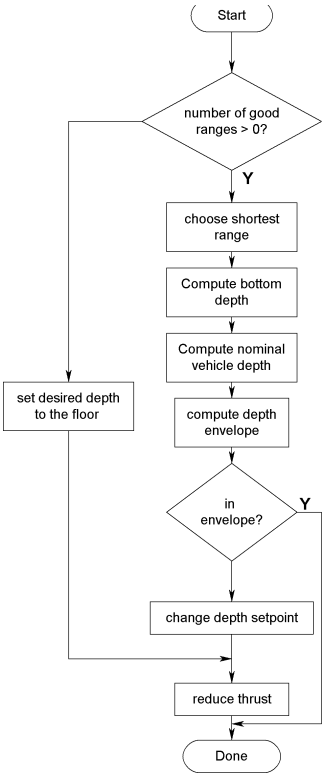

Fig. 5. ABE's bottom-following algorithm

of the total number of sensor measurements expected. The iterative implementation eliminates the need for batch processing of entire data sets, which often consist of $O\left(10^5\right)$ measurements per sensor.

The second tier consists of spatial groupings (clusters) of the selected measurements from the first tier. We use maximum inter-measurement distance as the criterion for cluster membership, set to twice the trackline spacing. Each stored measurement location is treated independently of its associated data type when deciding cluster membership. The algorithm then assigns a scalar value to each cluster that represents the relative value of revisiting the area circumscribed by that cluster (its revisitation-merit). The revisitation-merit of a cluster reflects both the ranking of its member measurements in their respective lists, and prior knowledge about the relative importance of each sensor in identifying hydrothermally altered water: first the filtered values stored in each list of selected measurements are normalized, then scaled according to data type, and finally summed to arrive at a scalar value for the cluster's revisitation-merit. Since the first tier of the algorithm consists of

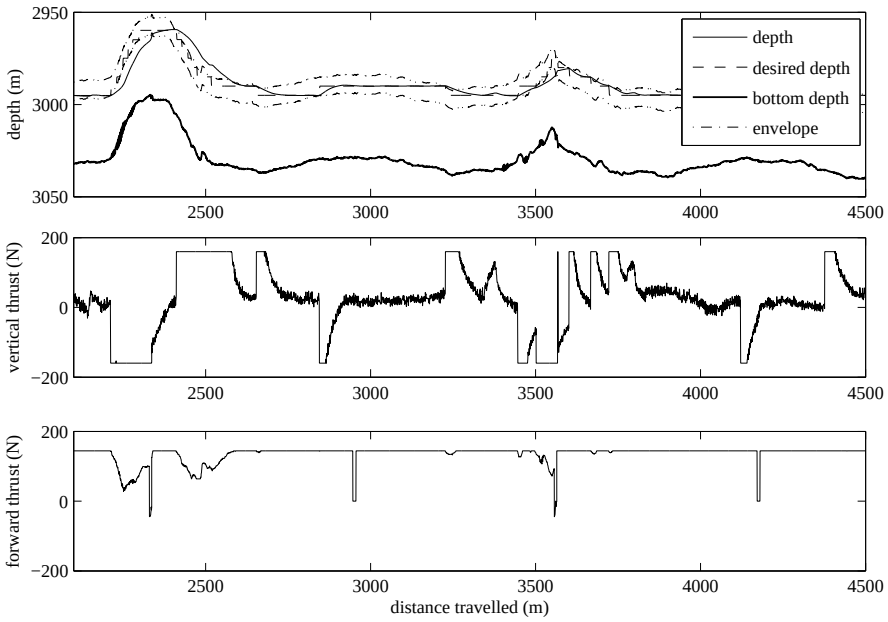

Fig. 6. Bottom following performance during a sonar survey at a height of 40 m: (**top**) vehicle depth, control envelope, and bottom trace as a function of distance traveled; (**middle**) vertical thrust; (**bottom**) forward thrust. These plots show that the bottom following algorithm (Fig. 5) makes infrequent adjustments to the commanded depth in mild terrain, driving with constant forward thrust and drawing only occasional bursts of vertical thrust

only a small fraction of the total data acquired, the computational costs of clustering are modest.

Thus far our approach to autonomous survey design based on these maps has been conservative. We have predefined the extent, spacing, and orientation of additional tracklines, leaving only absolute position to be determined in real-time as the centroid of the highest ranked cluster. Other procedures for autonomous survey design based on these maps might for instance define survey extent to cover member points such that some fraction total cluster value is included, or such that survey bounds completely encompass a cluster. These alternate strategies transfer much more of the onus of data-driven survey design to the vehicle and we anticipate they will improve performance by virtue of more tightly coupling data and trajectory generation.

Our strategy requires that an AUV survey an entire site to first build a map of high-revisitation-merit features before it makes any autonomous decisions. This approach to nested survey permits the vehicle to focus on the most interesting features, rather than relying on careful design of a threshold [16] to trigger pursuit of all potentially interesting features as they are encountered.

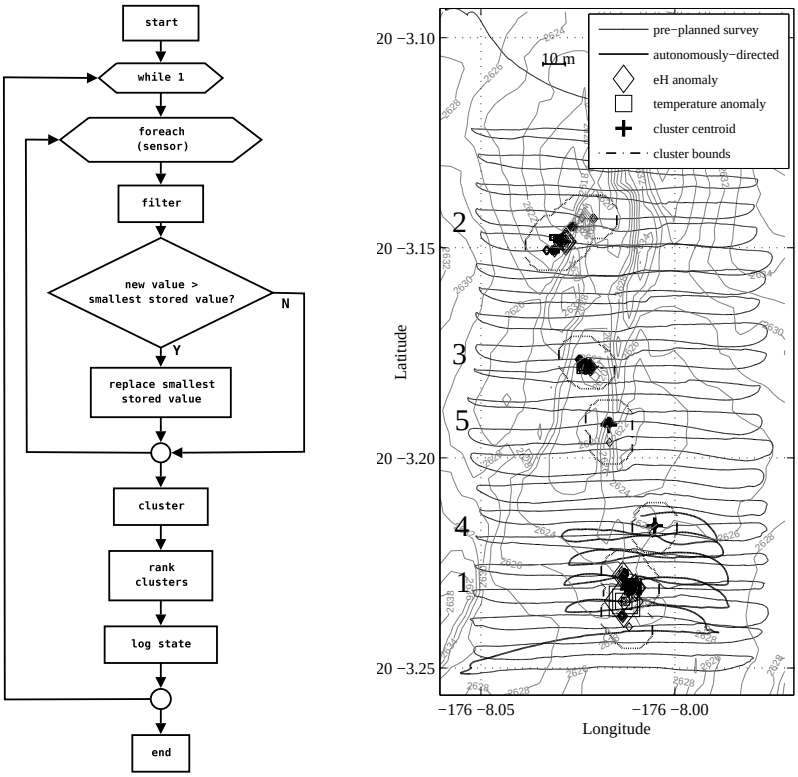

Fig. 7. Mapping in support of automated nested survey: (**left**) flowchart depicting the maintenance of sorted lists of selected measurements from multiple sensors, clustering by measurement location, and the ranking of the resulting clusters; (**right**) ranked clusters of selected hydrographic measurements. The map is shown just before the start of the autonomously directed portion of the dive. The size of each mark indicates the relative intensity of that sample

For the problem of detecting and locating hydrothermal vents, our approach may require the vehicle to cover more ground than a triggered approach would; however, the vehicle is less likely to spend time exploring false alarms or low-value targets.

To date we have applied our methodology to a total of four near-bottom photo-survey dives on two expeditions with ABE (ELSC and SMAR). Of these four dives, three returned with additional photographs of vent structures and associated fauna. A camera problem prevented the single unsuccessful survey from returning any photographs at all, but even after careful scrutiny of the intact data from the dive, the autonomously-directed portion of the unsuccessful dive became the basis of a subsequent preplanned dive. The right panel of Fig. 7 shows example results from a dive to a hydrothermal site on the ELSC. The output of the mapping algorithm is shown at the conclusion

of the preplanned portion of the dive along with the autonomously-directed portion of the dive. The latter portion comprised only 5% of total dive time, yet it yielded a 36% increase in the number of photographs with high scientific value.

Our goal on future expeditions is to apply the same map-based strategy to automate the sequence of successively higher resolution and lower altitude surveys currently employed to find hydrothermal vent sites on the seafloor with ABE (Fig. 1(a)).

6 Conclusion

We describe a set of algorithms that have been successfully used in the field with our autonomous underwater vehicle, ABE. We present our algorithm for processing acoustic long baseline returns that enables the vehicle to reliably determine its position despite the non-Gaussian noise properties of the data. We report on the algorithm that permits ABE to follow the seafloor even in very rugged terrain. Finally we report on an algorithm for automated, nested survey that permits ABE to automatically revisit sites of high interest.

We have used ABE, enabled by these algorithms, to build detailed sonar maps and photomosaics, and to locate and characterize deep sea hydrothermal vent sites. These mapping results have yielded scientifically significant data in their own right, and have enabled follow-up expeditions using remotely operated vehicles to efficiently perform detailed survey and sampling.

Acknowledgment

We thank our collaborators in the deep sea scientific community for envisioning innovative uses for ABE, and especially for recognizing its potential to provide new scientific insights unavailable or difficult to acquire through other means. In particular we gratefully acknowledge the continued support of Drs. Russell McDuff, John Delaney, Deborah Kelley, Timothy Shank, Christopher German, and Charles Langmuir. Work herein was supported by the National Science Foundation (OCE-0241913) and the National Oceanic and Atmospheric Administration (NA030AR4600115).

References

1. Fornari D, Tivey M, Schouten H, et al. (2004) Submarine lava flow emplacement processes at the East Pacific Rise 9°50′ N: Implications for hydrothermal fluid circulation in the upper ocean crust. In: German C, Lin J, Parson LM (eds) The Thermal Structure of the Ocean Crust and Dynamics of Hydrothermal Circulation. AGU Geophysical Monograph 148(31)

2. Tivey MA, Johnson HP, Bradley AM, Yoerger DR (1998) Thickness of a submarine lava flow determined from near-bottom magnetic field mapping by autonomous underwater vehicle. Geophys Res Lett 25(6):805–808
3. Cormier M-H, Ryan WBF, Shah A, et al. (2003) Waxing and waning volcanism along the East Pacific Rise on a millenium timescale. Geology 31(7):633–636
4. Schouten H, Tivey M, Fornari D, et al. (2003) Central anomaly magnetization high: Constraints on the volcanic construction and architecture of young upper oceanic crust, EPR 9–10° N. Ridge 2000 Events 1:30–34
5. Carbotte SM, Ryan WBF, Jin W, et al. (2003) Magmatic subsidence of the EPR at 18°14′ S revealed through fault restoration of ridge crest bathymetry. Geochem Geophy Geosyst 4(1):1008, doi:10.1029/2002GC000337
6. Kelly DS, Karson JA, Früh-Green GL, et al. (2005) A serpentinite-hosted ecosystem: The Lost City hydrothermal field. Science 307(5714):1428–1434
7. Stahr F, McDuff R, Yoerger D, Bradley A, Nakamura K (2000) Heat flux measurements at the Main Endeavour Vent Field, Juan de Fuca Ridge. In: Eos Trans AGU, Fall Meet Suppl 81(48), Abstract OS52I-03
8. Yoerger DR, Bradley AM, Stahr F, McDuff R (2001) Surveying deep-sea hydrothermal vent plumes with the Autonomous Benthic Explorer (ABE). In: Proceedings of the 12th International Symposium on Unmanned Untethered Submersible Technology
9. Langmuir CH, German C, Michael P, et al. (2004) Hydrothermal prospecting and petrological sampling in the Lau Basin: Background data for the Integrated Study Site. Eos Trans AGU, Fall Meet Suppl 85(47), Abstract B13A-0189
10. German CR, Connelly DP, Prien RG (2005) New techniques for hydrothermal plume investigation by AUV. Geophys Res Abs, EGU General Assembly, Abstract EGU05-A-04361
11. Nakamura K, Veirs S, Sarason CP, et al. (2000) Electrochemical signals in rising buoyant plumes and tidally oscillating plumes at the Main Endeavour Vent Field, Juan de Fuca Ridge. In: Eos Trans AGU, Fall Meet Suppl 81(48), Abstract OS52I-05
12. Pizarro O, Singh H (2003) Toward large area mosaicing for underwater scientific applications. IEEE J Ocean Eng 28(4):651–672
13. Hunt MM, Marquet WM, Moller DA, Peal KR, Smith WK (1974) An Acoustic Navigation System. Tech Rep WHOI-74-6, Woods Hole Oceanographic Institution, Woods Hole, Massachusetts
14. Milne PH (1983) Underwater Acoustic Positioning Systems. Gulf Publishing Company, Houston
15. Deffenbaugh M, Schmidt H, Bellingham JG (1996) Acoustic positioning in a fading multipath environment. In: Proceedings IEEE/MTS Oceans'96:596–600
16. Camilli R, Bingham B, Jakuba M, Singh H, Whelan J (2004) Integrating in situ chemical sampling with AUV control systems. In: Proceedings Oceans'04 MTS/IEEE Techno-Ocean'04 1:101–109